Molecular Therapy
Methods & Clinical Development
Original Article

Wound Healing Properties of Histatin-5 and Identification of a Functional Domain Required for Histatin-5-Induced Cell Migration

Dhara Shah,[1] Kyung-No Son,[1] Sushma Kalmodia,[1] Bao-Shiang Lee,[2] Marwan Ali,[1] Arun Balasubramaniam,[1] Deepak Shukla,[1,3] and Vinay Kumar Aakalu[1]

[1]Department of Ophthalmology and Visual Sciences, University of Illinois at Chicago, Chicago, IL, USA; [2]Research Resources Center, University of Illinois at Chicago, Chicago, IL, USA; [3]Department of Microbiology and Immunology, University of Illinois at Chicago, Chicago, IL, USA

Histatin peptides are endogenous anti-microbial peptides that were originally discovered in the saliva. Aside from their broad anti-microbial properties, these peptides play an important role in multiple biological systems. Different members of this family are thought to have relative specializations, with histatin-5 originally being thought to have mostly anti-fungal properties, and histatin-1 having strong wound healing properties. In this report, we describe the robust wound healing properties of histatin-5 and elucidate a functional domain, which is necessary and sufficient for promoting wound healing. We demonstrate these findings in multiple different cell types *in vitro* and with a standardized murine corneal wound healing model. Discovery of this wound healing domain and description of this functional role of histatin-5 will support developing therapies.

INTRODUCTION

Wound healing and epithelial migration are important areas of study for numerous biological systems. Histatins are an important family of endogenous anti-microbial peptides with numerous biological actions, including anti-microbial, immunomodulatory, and pro-wound healing effects.[1] We recently reported that histatin-1 (Hst1) can promote wound healing in human corneal epithelia, and these findings have been corroborated in rabbit models of corneal wounding *in vivo*.[2,3] The family of histatins contains two genes (*HTN1* and *HTN3*) and 13 protein products. Hst1, Hst2, and Hst3, but not Hst5, are thought to have wound healing properties attributed to their C-terminal.[1,4] The minimal active wound healing domain of Hst1 (residues 20–32; SHREFPFYGDYGS) was determined using scratch assays and serial truncation experiments. Hst5 is a proteolytic product of Hst3. The C terminal of Hst5 retains only the SHR of the wound healing domain of Hst1 (Figure 1).[1,4,5]

Saliva has pro-wound healing and anti-microbial effects. In small animals, it is thought that epidermal growth factor (EGF) is the primary contributor to the wound healing effects of saliva. In humans, Oudhoff et al.[4,5] have demonstrated that EGF and Hst1 can similarly enhance epithelial migration, but that Hst1 and other histatins are present at much higher concentrations than EGF. It has also been demonstrated that the wound healing effects of some histatins are sensitive to mitogen-activated protein kinase (MAPK) inhibition but not to EGF blockade. Notably, Hst2 induced wound healing is sensitive to extracellular signal-regulated kinase 1/2 (ERK1/2) inhibition but not p38 inhibition. Histatins have also been demonstrated to have pro-migratory effects in multiple different cell types.[1,2,4,5] We have recently demonstrated that histatins are an important part of the ocular surface, being present in the tear-producing lacrimal gland, promoting corneal epithelial migration and being a potential biomarker for ocular surface dry eye diseases such as Sjögren's syndrome and ocular graft-versus-host disease, suggesting a broader role for these peptides than originally thought.[2,6,7]

With the understanding that histatin peptides are an important part of the wound healing apparatus in multiple different epithelial tissues, and augment a growing understanding of the contribution of this peptide family to the ocular surface, we sought to determine whether Hst5 could promote wound healing in multiple cellular systems. We also sought to determine whether there was a domain in Hst5 that underpinned any of the potential pro-migratory effects of Hst5.

RESULTS

Hst5 Promotes Cell Migration

In order to determine whether Hst5 could promote epithelial cell migration, we performed a cell sprouting assay using human corneal epithelial (HCE) cells embedded as a spot in Cultrex. Sequences of peptides used in this study are shown in Figure 1. Interestingly, we found an increase in cell migration in the Hst5 (50 μM)-treated condition compared to the untreated (Un) control at 72 h (Figure 2). Next, to gain further confidence in our results, we corroborated these findings in a human corneal limbal epithelial (HCLE) cell line.[2] To test the effects of Hst5 on cell migration, HCLE cells were grown to

Received 3 February 2020; accepted 25 March 2020;
https://doi.org/10.1016/j.omtm.2020.03.027.

Correspondence: Kumar Aakalu, MD, Department of Ophthalmology and Visual Sciences, University of Illinois at Chicago, 1855 West Taylor Street, MC 648, Suite 3.158, Chicago, IL 60612.
E-mail: vaakalu@uic.edu

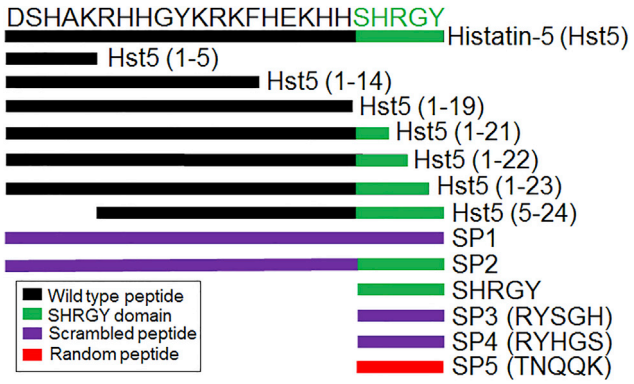

Figure 1. Schematic Description of Peptides

Peptides used in this study are depicted including histatin-5 (Hst5) and truncated variants with remaining residues indicated in parentheses (*x–y*). The SHRGY sequence, or remainder of the SHRGY sequence, is depicted in green. Scrambled peptide (SP) variants are depicted. SP1 and SP2 are 24 aa (full length of Hst5), and native sequence used for scrambling is indicated in purple. SP3 and SP4 are scrambled versions of SHRGY. SP5 is a random pentapeptide with similar charge characteristics and molecular weight to SHRGY and is shown in red.

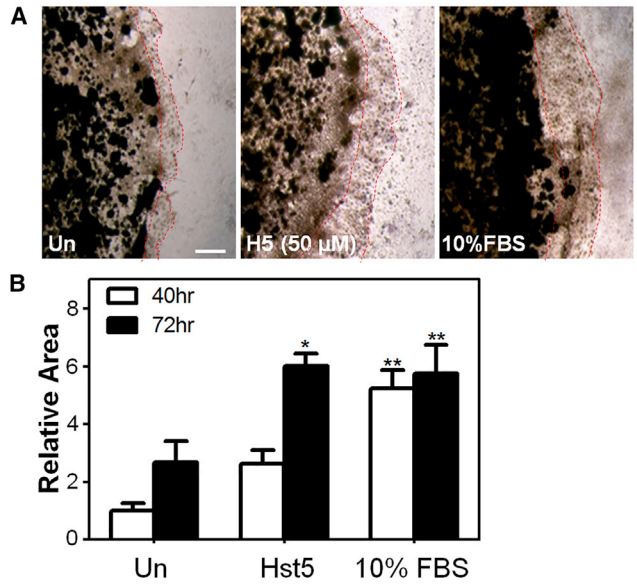

Figure 2. Histatin-5 Promotes Migration of Human Corneal Epithelial (HCE) Cells in a Sprouting Assay

A Cultrex-embedded spot of HCE cells (5×10^5/10 μL) was exposed to reduced serum media (untreated [Un] negative control), Hst5 (50 μM), or 10% FBS (positive control). (A) The size of the cellular spot was then followed and imaged at 72 h. Scale bar, 500 μm. (B) We found statistically significant expansion of spot size and extension of the HCE cells out of the Cultrex spot when exposed to Hst5 and FBS compared with Un at 72 h, suggesting that Hst5 can promote cellular migration in this assay. Statistical significance was determined by two-way ANOVA with a Bonferroni's *post hoc* test. *$p < 0.05$, **$p < 0.01$.

confluence and mechanically scratched using a pipette tip. Cells were then treated with a range of concentrations (20, 50, 80, and 100 μM) of Hst5 or Un. Time-lapse microscopy was performed and wound areas were analyzed at different time points. Figure 3 demonstrates a dose-dependent increase in the rate of scratch closure *in vitro* after the application of Hst5 compared to Un. The most significant increase in scratch closure was noticed at 50 μM. These findings were further corroborated in the HCE cell line with a statistically significant peak seen at 80 μM as compared with Un (Figure 4A). Moreover, similar results were also seen in disparate cell lines (HeLa cells and MCF-7 breast cancer cell line) (Figures 4B and 4C).

The SHRGY Domain of the C-terminal of Hst5 Is Critical for Promotion of Epithelial Cell Migration

To determine which portions of Hst5 were needed to promote epithelial cell migration, we performed a serial truncation experiment by progressively deleting residues in Hst5 and testing its efficacy. We found that the C-terminal SHRGY residues were necessary and sufficient to promote migration (Figure 5). All peptides were tested at 80 μM, based on our results in HCE cells (Figure 4A). Truncated versions of Hst5 that did not include the C terminus SHRGY sequence showed no significant increase in wound closure rates (Hst5 [1–5], Hst5 [1–14], Hst5 [1–19], Hst5 [1–21], Hst5 [1–22], Hst5 [1–23], scrambled peptide [SP] number 1 [SP1]) (Figure 5). However, constructs containing an intact SHRGY sequence (Hst5, Hst5 [5–24], SP2, SHRGY) showed significant increases in scratch closure rates (Figure 5). Scrambled peptides of SHRGY (SP3, SP4) did not increase wound closure rates. Moreover, SP5, a random pentapeptide with similar molecular weight and charge characteristics to SHRGY, showed no significant improvement in the wound closure rates (Figure 5). Thus, the SHRGY sequence is necessary and sufficient to promote epithelial migration rates in *in vitro* scratch assays.

Hst5 Enhances Cell Spreading

We then sought to determine whether cell spreading was enhanced in HCE cells after application of Hst5 peptide. Cell spreading was determined using multiple measurements of individual cells in low-density culture after Hst5 application and compared with Un. In addition, visualization of the cell actin skeleton was performed using phalloidin staining. Figure 6 demonstrates a statistically significant increase in cell surface area after application of Hst5 compared with control.

ERK Activation Is Necessary for the Pro-migratory Effects of Hst5

In order to determine whether the cellular signaling pathways underpinning the pro-migratory effects of Hst5 were similar to those of Hst1 in other epithelial cell types, we investigated the level of activation/phosphorylation of ERK with and without wounding and with and without Hst5 application. We used immunolocalization to determine whether Hst5 application to a scratched sheet of epithelium would affect phosphorylated (p)ERK1/2 levels (Figure 7A). We corroborated these findings using western blotting (WB) and found that wounding increased pERK1/2 levels alone, and that these levels were further increased by Hst5 application (Figure 7B).

We then tested the hypothesis that SHRGY-containing variants of Hst5 were necessary for the increase in pERK1/2. We found that

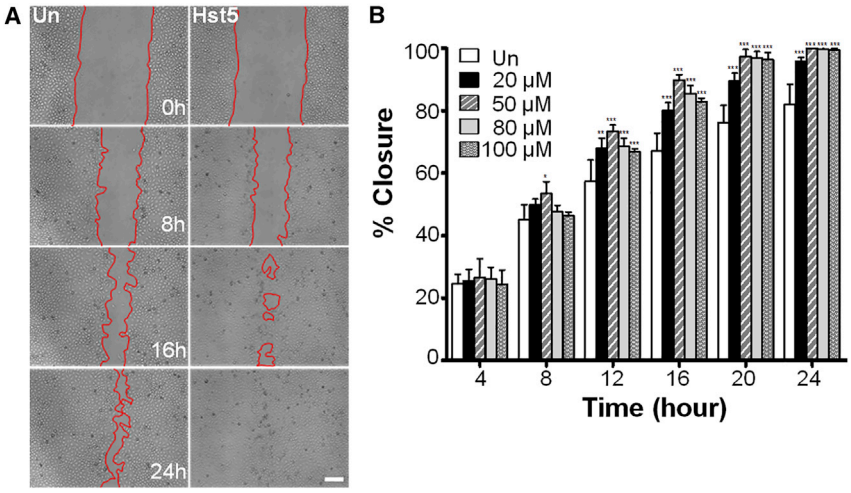

Figure 3. Histatin-5 Accelerates Human Corneal Limbal Epithelial (HCLE) Cell Migration in Standardized Scratch Assays

(A) Time-lapse microscopy (ImageXpress Micro, Molecular Devices, San Jose, CA, USA) at ×4 magnification, after standardized wounding of confluent HCLE cells in serum-free conditions, was used to quantify migration rates and scratch closure times with and without Hst5 co-treatment at the time of wounding. Scale bar, 200 μm. (B) Bar graph depicting scratch closure percentage over time. Notably, we found a statistically significant improvement in scratch closure rates (versus Un control) at all concentrations at 12 h and after. 50 μM was significantly better than 20 μM at 16 and 20 h, and concentrations above 50 μM did not improve scratch closure rates better than 50 μM, suggesting that the peak dose in the tested range for HCLE cells was 50 μM. A similar experiment was performed with HCE cells with a peak effect at 80 μM (Figure 4A). All experiments were performed three separate times with three technical replicates for each experiment. Statistical significance was determined by two-way ANOVA with a Bonferroni's *post hoc* test. *p < 0.05, **p < 0.01, ***p < 0.001. % closure = (scratch area at time 0 − scratch area at time *x*)/scratch area at time 0) × 100. Un, untreated.

application of the SHRGY-containing scrambled peptide, SP2, increased pERK1/2 levels to a comparable intensity to Hst5. As expected, SP1, which does not contain SHRGY, did not elicit a similar increase in pERK1/2 immunolocalization to SHRGY-containing peptides (Figure 7A).

Next, we tested whether ERK activation was necessary for the wound healing effects of Hst5 using the ERK pathway inhibitor PD98059 (PD). We found that co-treatment of Hst5 and PD eliminated the effects of Hst5 on promoting wound closure, suggesting that Hst5 effects require ERK activation, which is consistent with our immunolocalization findings and the literature on corneal epithelial migration and histatin peptides in general (Figure 7C).[4,8]

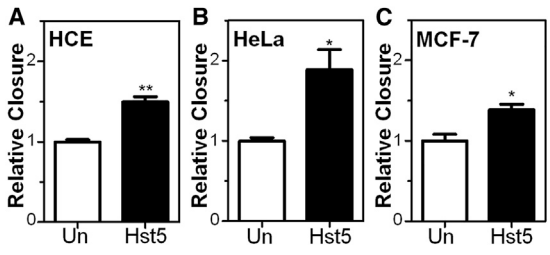

Figure 4. Histatin-5 Accelerates Cell Migration in Standardized Scratch Assays in Multiple Cell Types

Hst5 application led to statistically significant improvement in scratch closure rates in all tested cell types compared to Un controls. (A–C) Cell types and conditions used included (A) HCE cells, (B) HeLa cells, and (C) MCF-7 cells in reduced serum conditions. All experiments were performed three separate times with three technical replicates for each experiment. Statistical significance was determined using the Student's t test. *p < 0.05, **p < 0.01. Relative closure = (% closure of treated sample)/(% closure of Un control).

Hst5 Application Promotes Wound Healing in a Murine Corneal Injury Model

These *in vitro* results encouraged us to further explore Hst5 in a murine corneal epithelial injury model. Using a standard mouse model of corneal injury, topical application of Hst5 or SHRGY significantly increased wound healing rates compared with SP1 (Figures 8A and 8B). Histological analysis of the wounded corneas (DAPI staining on the cross-sections of the cornea) (Figure 8C) demonstrated pathologic evidence of reductions in corneal wound size in the Hst5-treated condition compared to SP1-treated controls. Thus, Hst5- and SHRGY-containing peptides can enhance wound healing in a well-vetted model of murine corneal epithelial injury.

DISCUSSION

In this study, we report for the first time that the SHRGY pentapeptide alone or as a domain of Hst5 is necessary and sufficient to promote epithelial migration and ERK activation *in vitro*, and corneal wound healing *in vivo*. This study also advances the literature by confirming the pro-wound healing and epithelial migration enhancing effects of Hst5 in multiple human cell types. Given the broad importance of epithelial migration to wound healing, regenerative therapies, and homeostatic mechanisms in multiple biological systems, we think that these findings have implications in multiple fields.

Although they were originally described in saliva, histatins have since been found in the ocular surface, tear film, and lacrimal gland and reported to be elaborated by a number of cancer cell lines, highlighting their importance in multiple biological systems.[1,7,9] Aside from their importance in preventing infection in the oral cavity, they may have relevance as biomarkers of ocular and other diseases, including dry eye disease.[7] Oudhoff et al.[4,5] originally reported the wound healing and pro-migratory effects of many histatin peptides, but they did not find significant improvement in wound healing rates with Hst5.

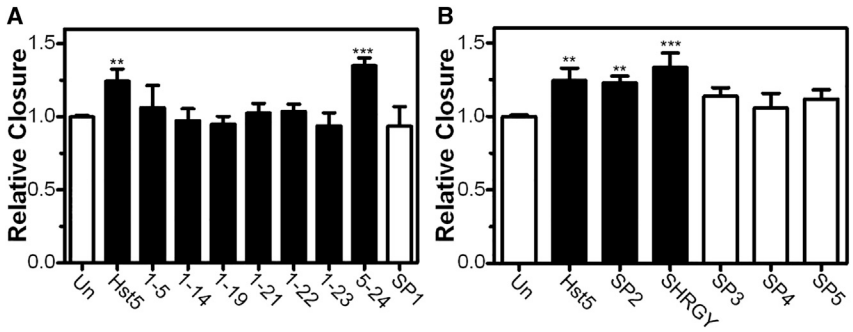

Figure 5. SHRGY-Containing Peptides Are Necessary and Sufficient for Acceleration of Scratch Closure Rates

(A and B) Hst5 peptides containing SHRGY sequences and truncated forms were tested for efficacy in accelerating scratch closure rates. Negative controls included Un and multiple SP controls. Notably, application of peptides containing intact C-terminal SHRGY (Hst5, Hst5 [5–24], SP2) and SHRGY all promoted statistically significant improvements in scratch closure rates, whereas application of any peptides that did not contain SHRGY (Hst5 [1–5], Hst5 [1–14], Hst5 [1–19], Hst5 [1–21], Hst5 [1–22], Hst5 [1–23]) and negative controls (Un and SP1) did not accelerate scratch closure. Additionally, scrambled versions of SHRGY (SP3, SP4) and SP5 also failed to accelerate rates of scratch closure. Taken together, these results suggest that the sequence of SHRGY is important and that a pentapeptide of similar charge and size does not have similar effects on wound closure rates. All peptides were tested at 80 μM. All experiments were performed three separate times with three technical replicates for each experiment. Statistical significance was determined by one-way ANOVA with a Dunnett's *post hoc* test. $^{**}p < 0.01$, $^{***}p < 0.001$. Relative closure = (% closure of treated sample)/(% closure of Un control). Scratch closure rates in response to treatment with peptides containing SHRGY (Hst5, SP2, SHRGY) and scrambled pentapeptides (SP3, SP4, SP5) (panel B) are separated from truncated peptides (panel A) for clarity.

Very recently, a group reported that modification of Hst5 to reduce proteolytic activity by *Candida albicans* had the unexpected effect of increasing oral keratinocyte migration rates.[10]

Peptide therapeutic design can be informed by detailed understanding of native domain functionality. Oudhoff et al.[4,5] performed a series of classical truncation experiments to determine the critical wound healing domain in Hst1 and other histatins. Understanding the functional domains of histatins that are responsible for effects on human cell types is critically important for understanding the mechanisms of these effects.

In this study, we demonstrate in multiple cell types that Hst5 can indeed promote cell migration, with similar effect sizes to other histatin peptides and that the SHRGY domain is necessary and sufficient for these effects. The importance of this domain is also seen in the necessity of the SHRGY domain for activation of ERK1/2. Excitingly, the demonstrated effects of Hst5 increased wound healing *in vitro*, and the importance of the SHRGY domain for these effects translated to increased wound healing rates *in vivo*. Moreover, similar to Hst1, Hst5 appears to cause an increase in cell spreading.

Developing new therapies on the basis of these results, while exciting, should be carried out only after understanding the limitations of this early work. Future study into the mechanisms of action and cellular interactors for Hst5 will be needed to better understand the physiology underpinning the findings in the present study. Cellular and animal models of wound healing and epithelial migration should be corroborated in large animal models and in multiple biological systems. That being said, we have utilized multiple different cell types (two different corneal cell lines, and non-corneal lines HeLa and MCF7), lending support to the generalizability of our findings. Moreover, corneal epithelial injury is a standard wound healing model that has been used by many investigators.[11,12] Additionally, toxicological testing and larger dose-finding experiments will be necessary for translational application of these results. Finally, while our study demonstrated a significant effect in multiple experiments, with similar effect sizes to those seen by other investigators in Hst1 studies, and several controls were used, generalizability of these findings will require independent validation by other research groups.[4]

MATERIALS AND METHODS

Peptide Synthesis

Hst5 peptides were synthesized using standard Fmoc-based solid-phase synthesis chemistry on a Symphony peptide synthesizer (Protein Technologies, Tucson, AZ, USA). The first amino acids (Fmoc-Tyr-OH) was covalently attached to the Wang resin. The peptide was synthesized in cycles, starting with the removal of the Fmoc group in 20% piperidine in *N*,*N*-dimethylformamide (DMF). The next amino acid was coupled using 0.1 M 2-(1*H*-benzotriazole-1-yl)-1,1,3,3-tetramethyluronium hexafluorophosphate (HBTU) in DMF containing 0.4 M 4-methyl morpholine for 30 min (twice), and this process was continued to complete the synthesis. The resin-bound peptide was deprotected and cleaved from the resin using trifluoroacetic acid (TFA). Ethyl ether was added to precipitate the peptide from the TFA solution. The precipitated peptide was then dissolve in 50% acetonitrile in water and lyophilized. The crude peptide was purified on a Kinetex reversed-phase C18 column, 150 × 21.1 mm (Phenomenex, CA, USA), using a BioCad Sprint (Applied Biosystems, Foster City, CA, USA) high-pressure liquid chromatography (HPLC) system. The pure peptide fraction was identified by electrospray ionization mass spectrometry (ESI MS) and lyophilized as appropriate.

The peptides were dissolved in cell culture grade water to obtain stock concentration of 10 mM and were stored at −20°C. Scrambled peptides were designed in conjunction with Protein Research Lab (PRL) at the University of Illinois at Chicago (UIC). Table 1 shows the sequences of all peptides used in this study.

Cell Culture

HCLE cells were cultured in keratinocyte serum-free medium (KSFM) (Thermo Scientific, Waltham, MA, USA) supplemented with 0.2 ng/mL recombinant human EGF (rhEGF) (Thermo

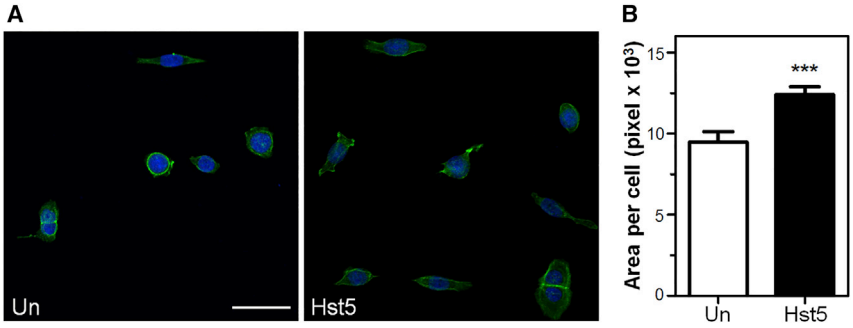

Figure 6. Histatin-5 Enhances Cell Spreading

A cell spreading assay using cell surface area measurements and visualization of actin in HCE cells via phalloidin staining is shown. Noted is the statistically significant increase in cell surface area after application of Hst5 compared with Un control. (A) Representative images of HCE cell spreading 24 h after seeding in the presence or absence of Hst5. Green shows actin; blue shows nuclei. Scale bar, 50 μm. (B) The average surface area per cell was quantified from images similar to those in (A). Measurement of average individual cell surface area is significantly higher with Hst5 treatment compared with Un. Statistical significance was determined by using the Student's t test. ***$p < 0.001$. The error bar represents means ± SEM (n = 40 cells measured per treatment condition).

Scientific, Waltham, MA, USA), bovine pituitary extract (Thermo Scientific, Waltham, MA), and 1% amphotericin B (Thermo Scientific, Waltham, MA, USA). Standard cell culture conditions (37°C, 5% CO_2, >95% humidity) were used during routine passages, as has been done previously.[13] The culture medium was replaced every 48 h after seeding.

HCE cells were cultured in a minimum essential medium (MEM) (Gibco/Life Technologies, Carlsbad, CA, USA). HeLa cells were maintained in Dulbecco's modified Eagle's medium (DMEM) (Life Technologies, Grand Island, NY, USA), and both media were supplemented with 10% fetal bovine serum (FBS) (Gibco/Life Technologies, Carlsbad, CA, USA) and 1% penicillin-streptomycin (Gibco/Life Technologies, Carlsbad, CA) as reported previously.[14,15] MCF-7 cells were cultured in Roswell Park Memorial Institute (RPMI) 1640 (Gibco, Grand Island, NY, USA) supplemented with 10% FBS (Gibco/Life Technologies, Carlsbad, CA, USA) and 1% penicillin-streptomycin (Gibco/Life Technologies, Carlsbad, CA). Standard cell culture conditions (37°C, 5% CO_2, >95% humidity) were used during routine passages, as has been done previously.[16]

Cell Sprouting Assay

A cell sprouting assay was performed using HCE cells in Cultrex (Trevigen, Gaithersburg, MD, USA) (reduced and diluted in MEM at 1:1). HCE cells were embedded in Cultrex at 5×10^5 cells/10 μL of spot, then dried in an incubator for 45 min, followed by the addition of media with treatment or control. The cell-spotted plates were then exposed to reduced serum media (0.5% FBS) (Un negative control), Hst5 (50 μM), or 10% FBS (positive control). The Cultrex-embedded spots were then imaged at 40 and 72 h using an inverted light microscope (DMi1, Leica Microsystems, Buffalo Grove, IL, USA) at ×4 magnification. The cellular spot-covered area at each time point was measured using ImageJ v1.47 software (NIH, Bethesda, MD, USA). At 72 h, cells were fixed using methanol for 20 min and stained with trypan blue dye (Lonza, Basel, Switzerland).

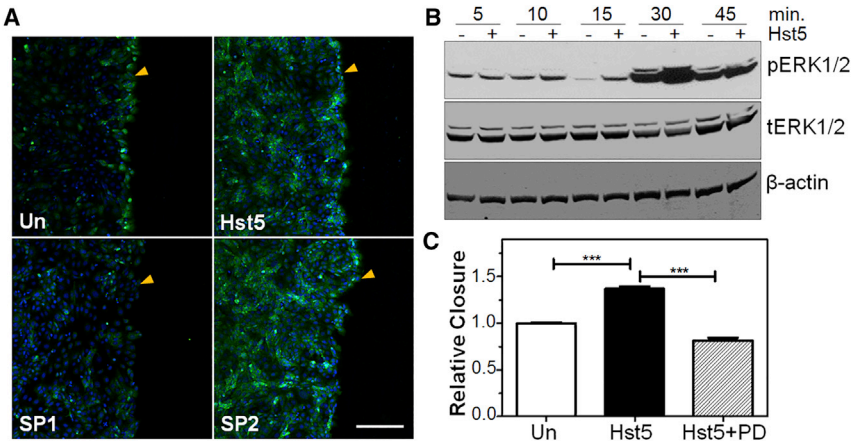

Figure 7. Histatin-5-Induced Wound Healing Is ERK1/2-Dependent

(A) Immunolocalization of pERK1/2 in Un (+scratched) HCE cells demonstrates localization of pERK1/2 to the wounded edge of the epithelial monolayer. Application of Hst5 or SHRGY containing peptide (SP2) increases signal intensity of pERK1/2 throughout the epithelial monolayer, whereas SP1 does not. Included images are representative of multiple images taken per sample from duplicate experiments and at multiple time points. All peptides used were applied at 80 μM. Arrowheads indicate wound edge. Scale bar, 200 μm. (B) Western immunoblotting (WB) analysis of ERK1/2 phosphorylation/activation. Scratching and treatment with Hst5 increases pERK1/2 activation after 30 min compared with Un control. (C) Acceleration of scratch closure by histatin-5 is sensitive to ERK inhibition. ERK1/2 inhibitor PD was applied to determine whether Hst5 induced scratch closure acceleration depends on ERK1/2 activation. Tested groups included Un, Hst5 (80 μM), and Hst5 (80 μM) + PD (50 μM) co-treatment at the time of wounding. We found a statistically significant improvement in scratch closure rates with Hst5 compared to Un. Hst5 + PD co-treatment abrogated this effect, suggesting that the effects of Hst5 are sensitive to the actions of PD. All experiments were performed three separate times with three technical replicates for each experiment. Statistical significance was determined by a one-way ANOVA with a Bonferroni's *post hoc* test. ***$p < 0.001$. Relative closure = (% closure of treated sample)/(% closure of Un control).

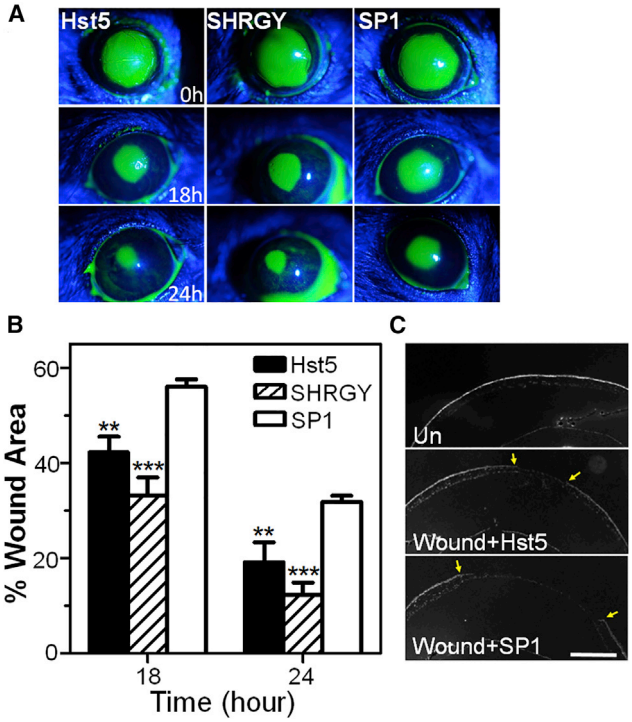

Figure 8. Application of Histatin-5 or SHRGY Peptides Accelerates Corneal Wound Closure Rates in a Murine Corneal Epithelial Injury Model

(A) Slit-lamp biomicroscopic images of murine corneas using a cobalt filter and fluorescein dye staining of the wounded areas are shown among the experimental groups (n = 7 for each group) (Hst5 [80 μM], SHRGY [80 μM], or SP1 [80 μM]). (B) Wound areas at multiple time points were measured using ImageJ software. Measurement of percentage remaining corneal wound area at 18 and 24 h compared to baseline showed statistically significant improvement in Hst5 and SHRGY groups compared to SP1. (C) DAPI stained cross-sections of the murine cornea and anterior segment of the eye show the reduction in size of the epithelial wound at 24 h in Hst5-treated mice compared with SP1 control mice. Wounded area is shown by arrowheads. Scale bar, 500 μm. Statistical significance was determined by a two-way ANOVA with Bonferroni's *post hoc* test. $^{**}p < 0.01$, $^{***}p < 0.001$. % Wound area = (wound area at time *x*/wound area at time 0) × 100.

In Vitro Scratch Assay

HCE, HCLE, HeLa, and MCF-7 cells were cultured in a 24-well plate at 2.5×10^5 cells/well seeding density and were grown to confluence on a 24-well plate. Subsequently, a straight line scratch mark was made with a sterile P200 pipette tip as described previously.[2] The cells were then washed twice with phosphate-buffered saline (PBS) to remove cellular debris. Wounded areas were then treated with Hst5, truncation forms, pentapeptide versions, and SP controls at various concentrations in standard media with reduced serum conditions (0.5% FBS in MEM [HCE], growth factor-free KSFM [HCLE], 1% FBS in DMEM [HeLa], and 0.5% FBS in RPMI 1640 [MCF-7]). Scratches were imaged microscopically at ×4 magnification (ImageXpress Micro, Molecular Devices, San Jose, CA, USA) every hour during the course of the experiment. The wound areas were measured using ImageJ v1.47 software (NIH, Bethesda, MD, USA). Relative wound closure was calculated by dividing the closure of the treated wound by that of the Un control wound.[5] For all of the truncation experiments Hst5 at a final concentration of 80 μM was used. PD98059 (Calbiochem, San Diego, CA, USA), a specific inhibitor of ERK1/2, at final concentration of 50 μM was added to cell cultures at the same time as histatin peptides.[8]

Cell-Spreading Assay

A cell-spreading assay was performed as previously reported.[2,5] HCE cells were trypsinized and subsequently seeded at low density so that a single-cell population prevailed. The cells were seeded with or without Hst5 (50 μM), and after 24 h they were fixed with 4% paraformaldehyde in PBS for 20 min and permeabilized with Triton X-100 (0.1%) in PBS for 5 min. Then, the cells were incubated with Oregon green 488 phalloidin (Thermo Fisher Scientific, Waltham, MA, USA) for 1 h for F-actin staining and DAPI for 10 min for nuclei staining. Images of the stained HCE cells were captured and analyzed using a Zeiss LSM 710 confocal microscope. The area of the individual cells (n = 40 per treatment condition) on phase-contrast images was calculated using ImageJ v1.47 software (NIH, Bethesda, MD, USA).

Mouse Model of Corneal Epithelial Wound Healing

Corneal wounding experiments in mice were conducted in compliance with the Association for Research in Vision and Ophthalmology (ARVO) Statement for the Use of Animals in Ophthalmic and Vision Research. The protocol was approved by the UIC Animal Care and Use Committee. Twelve to 19-week-old C57BL/6J (Jackson Laboratory, Bar Harbor, ME, USA) mice were anesthetized with intraperitoneal injection of ketamine (100 mg/kg) and xylazine (5 mg/kg). After applying two drops of topical 0.5% proparacaine, a 2.0-mm area of the central epithelium was demarcated using a 2-mm disposable biopsy punch and removed by an AlgerBrush II (The Alger Company, Lago Vista, TX, USA). In the treatment (n = 7) or the control (n = 7) group, Hst5 (80 μM), SHRGY (80 μM), or SP1 (80 μM) was applied to the cornea three times a day. At 0, 18, and 24 h, the corneas were stained with fluorescein (FUL-GLO fluorescein sodium ophthalmic strips, Akorn, Lake Forest, IL, USA) and imaged using a Nikon FS-2 photo-slit lamp with a Nikon D200 camera (Nikon, Melville, NY, USA). At each indicated time point, the remaining wound areas were measured using ImageJ software and compared with the baseline wound area for each mouse, and the percentage of the remaining wound area was calculated for each time point.

Western Blot

Western blot was performed following standard methods. Briefly, 20 μg of protein lysate was boiled in NuPAGE lithium dodecyl sulfate (LDS) sample buffer (Invitrogen, Carlsbad, CA, USA) for 10 min and then subjected to electrophoresis on 12% NuPage bis-Tris gels (Invitrogen, Carlsbad, CA, USA), followed by transfer to nitrocellulose membranes (Amersham Protran, GE Healthcare, Pittsburgh, PA, USA). Membranes were then blocked with Tris-buffered saline containing 3% nonfat dry milk for 1 h and incubated with primary antibody against pERK1/2 or total (t)Erk1/2 (Cell Signaling Technology, Danvers, MA, USA) (1:1,000) overnight at 4°C. After washing in 0.05% Tris-buffered saline containing 0.05% Tween 20 (TBST),

Table 1. Sequences for Experimental Peptides

Name	Sequence
Hst5	DSHAKRHHGYKRKFHEKHHSHRGY
Hst5 (1–5)	DSHAK
Hst5 (1–14)	DSHAKRHHGYKRKF
Hst5 (1–19)	DSHAKRHHGYKRKFHEKHH
Hst5 (1–21)	DSHAKRHHGYKRKFHEKHHSH
Hst5 (1–22)	DSHAKRHHGYKRKFHEKHHSHR
Hst5 (1–23)	DSHAKRHHGYKRKFHEKHHSHRG
Hst5 (5–24)	RHHGYKRKFHEKHHSHRGY
SHRGY	SHRGY
SP1	YHGHRHFRKHKKHKEAHSYDRGSH
SP2	HSHKEGHHYKRFKRKHHADSHRGY
SP3	RYSGH
SP4	RYHGS
SP5	TNQQK

Hst5, histatin-5.

membranes were then incubated for 1 h with goat anti-rabbit-horseradish peroxidase (HRP) (BD Biosciences, San Jose, CA, USA) (1:2,000) as the secondary antibody. The membranes were then developed using X-ray film and enhanced chemiluminescence (ECL) Pro solution (PerkinElmer, Waltham, MA, USA). β-Actin was used as an internal control.

Immunofluorescence Imaging

HCE cells were seeded in eight-well chamber slides at 9×10^4 cells/well seeding density and allowed to incubate to form a confluent monolayer. Subsequently, a straight-line scratch mark was made with a sterile P10 pipette tip. The cells were then washed with media to remove cellular debris. Wounded areas were then treated with Hst5, SP1, or SP2 and untreated at 80 μM concentrations in standard media with reduced serum conditions (0.5% FBS in MEM) for 45 min. Cells were then fixed with 4% paraformaldehyde for 30 min and permeabilized with 0.1% Triton X-100 for 5 min. After washing with PBS, cells were then incubated at room temperature for 30 min with 5% bovine serum albumin (BSA) and 5% normal goat serum in PBS. Cells were subsequently incubated with primary antibodies diluted in 1% BSA against pERK1/2 (1:200) (Cell Signaling Technology, Danvers, MA, USA) at 4°C for 16 h. After three washings with PBS, they were incubated with fluorescein isothiocyanate-conjugated sheep anti-rabbit immunoglobulin G (IgG) antibody (BD Biosciences, San Jose, CA, USA) (1:500) diluted in 1% BSA at room temperature for 60 min. After extensive washing with PBS, the cells were then stained with 4′,6-diamidino-2-phenylindole (DAPI) (Roche, Mannheim, Germany) for 2 min for nuclear staining. The cells were then mounted in Fluoro-Gel with Tris buffer (Electron Microscopy Sciences, Hatfield, PA, USA) and observed under a confocal microscope (LSM 710 confocal microscope, Zeiss, Oberkochen, Germany) using a ×10 objective.

For immunofluorescence, excised whole mouse eye was snap-frozen in optimal cutting temperature (OCT) compound (Fisher Healthcare, Waltham, MA, USA). The frozen tissues were cut into 10-μm cryosections (NX50 cryomicrotome, Thermo Fisher Scientific, Waltham, MA, USA), then sections were mounted on Superfrost Plus slides (Thermo Fisher Scientific, Waltham, MA, USA). Slides were fixed using methanol for 20 min, followed by several PBS washes and then stained with DAPI for 2 min for nuclear staining, followed by further washing with PBS and deionized water. The slides were then mounted in Fluoro-Gel with Tris buffer (Electron Microscopy Sciences, Hatfield, PA, USA) and observed using an upright microscope (Axioskop 2 Plus, Zeiss, Oberkochen, Germany) using a ×5 objective.

Statistical Analysis

Experiments were analyzed using two-way or one-way ANOVA followed by Bonferroni's or Dunnett's *post hoc* tests or the Student's t test, as appropriate. p values <0.05 were considered statistically significant. Statistical analyses were performed using GraphPad Prism 7.0 software (GraphPad, La Jolla, CA, USA).

AUTHOR CONTRIBUTIONS

Conceptualization: D. Shah, K.S., and V.K.A.; Methodology: D. Shah, K.S., and V.K.A.; Validation: D. Shah, K.S., and V.K.A.; Formal Analysis: D. Shah, K.S., V.K.A., A.B., and S.K.; Investigation: D. Shah, K.S., and V.K.A.; Resources: D. Shah, K.S., V.K.A., B.L., A.B., S.K., and M.A.; Data Curation: D. Shah, K.S., and V.K.A.; Writing – Original Draft: D. Shah, K.S., and V.K.A.; Writing – Review & Editing: D. Shah, K.S., V.K.A., D. Shukla, and M.A.; Visualization: D. Shah, K.S., and V.K.A.; Supervision: V.K.A.; Project Administration: A.B. and V.K.A; Funding Acquisition: V.K.A. and D. Shukla.

CONFLICTS OF INTEREST

V.K.A. is the co-inventor or inventor on multiple provisional and pending patents related to histatin peptides, owned by the Board of Trustees of the University of Illinois. The remaining authors declare no competing interests.

ACKNOWLEDGMENTS

This work was supported by the Department of Defense, Congressionally Directed Medical Research Program, Vision Research Program W81XWH-17-1-0122; Veterans Affairs Office of Research and Development grant I01BX004080; National Institutes of Health/National Eye Institute grants K08 EY024339, R01 EY029409, and P30 EY001792; and by an unrestricted grant from Research to Prevent Blindness (New York, NY, USA). The content is solely the responsibility of the authors and does not necessarily represent the official views of the National Institutes of Health, Department of Defense, or Veterans Affairs. The Graphical Abstract was made with the expert design assistance of Laruen Kalinoski. Peptide synthesis was performed through the Research Resources Center of the University of Illinois at Chicago (Chicago, IL, USA). The MCF-7 cell line was provided by Jonna Frasor (University of Illinois at Chicago, Chicago, IL, USA). HCE cells and HeLa cells were provided by Deepak Shukla (University of Illinois at Chicago, Chicago, IL, USA). HCLE cells

were provided by Sandeep Jain (University of Illinois at Chicago, Chicago, IL, USA).

REFERENCES

1. Torres, P., Castro, M., Reyes, M., and Torres, V.A. (2018). Histatins, wound healing, and cell migration. Oral Dis. *24*, 1150–1160.
2. Shah, D., Ali, M., Shukla, D., Jain, S., and Aakalu, V.K. (2017). Effects of histatin-1 peptide on human corneal epithelial cells. PLoS ONE *12*, e0178030.
3. Oydanich, M., Epstein, S.P., Gadaria-Rathod, N., Guers, J.J., Fernandez, K.B., and Asbell, P.A. (2018). In vivo efficacy of histatin-1 in a rabbit animal model. Curr. Eye Res. *43*, 1215–1220.
4. Oudhoff, M.J., Bolscher, J.G., Nazmi, K., Kalay, H., van 't Hof, W., Amerongen, A.V.N., and Veerman, E.C. (2008). Histatins are the major wound-closure stimulating factors in human saliva as identified in a cell culture assay. FASEB J. *22*, 3805–3812.
5. Oudhoff, M.J., Kroeze, K.L., Nazmi, K., van den Keijbus, P.A., van 't Hof, W., Fernandez-Borja, M., Hordijk, P.L., Gibbs, S., Bolscher, J.G., and Veerman, E.C. (2009). Structure-activity analysis of histatin, a potent wound healing peptide from human saliva: cyclization of histatin potentiates molar activity 1,000-fold. FASEB J. *23*, 3928–3935.
6. Shah, D., Ali, M., Pasha, Z., Jaboori, A.J., Jassim, S.H., Jain, S., et al. (2016). Histatin-1 expression in human lacrimal epithelium. PLoS One *11*, e0148018.
7. Kalmodia, S., Son, K.-N., Cao, D., Lee, B.-S., Surenkhuu, B., Shah, D., Ali, M., Balasubramaniam, A., Jain, S., and Aakalu, V.K. (2019). Presence of histatin-1 in human tears and association with aqueous deficient dry eye diagnosis: a preliminary study. Sci. Rep. *9*, 10304.
8. Sharma, G.-D., He, J., and Bazan, H.E. (2003). p38 and ERK1/2 coordinate cellular migration and proliferation in epithelial wound healing: evidence of cross-talk activation between MAP kinase cascades. J. Biol. Chem. *278*, 21989–21997.
9. Ali, M., Shah, D., Pasha, Z., Jassim, S.H., Jassim Jaboori, A., Setabutr, P., and Aakalu, V.K. (2017). Evaluation of accessory lacrimal gland in Muller's muscle conjunctival resection specimens for precursor cell markers and biological markers of dry eye disease. Curr. Eye Res. *42*, 491–497.
10. Sultan, A.S., Vila, T., Hefni, E., Karlsson, A.J., and Jabra-Rizk, M.A. (2019). Evaluation of the antifungal and wound-healing properties of a novel peptide-based bioadhesive hydrogel formulation. Antimicrob. Agents Chemother. *63*, e00888–e19.
11. Fernandes-Cunha, G.M., Na, K.S., Putra, I., Lee, H.J., Hull, S., Cheng, Y.C., Blanco, I.J., Eslani, M., Djalilian, A.R., and Myung, D. (2019). Corneal wound healing effects of mesenchymal stem cell secretome delivered within a viscoelastic gel carrier. Stem Cells Transl. Med. *8*, 478–489.
12. Reins, R.Y., Hanlon, S.D., Magadi, S., and McDermott, A.M. (2016). Effects of topically applied vitamin D during corneal wound healing. PLoS ONE *11*, e0152889.
13. Abdel-Naby, W., Cole, B., Liu, A., Liu, J., Wan, P., Guaiquil, V.H., Schreiner, R., Infanger, D., Lawrence, B.D., and Rosenblatt, M.I. (2017). Silk-derived protein enhances corneal epithelial migration, adhesion, and proliferation. Invest. Ophthalmol. Vis. Sci. *58*, 1425–1433.
14. Yakoub, A.M., and Shukla, D. (2015). Herpes simplex virus-1 fine-tunes host's autophagic response to infection: a comprehensive analysis in productive infection models. PLoS ONE *10*, e0124646.
15. Duggal, N., Jaishankar, D., Yadavalli, T., Hadigal, S., Mishra, Y.K., Adelung, R., and Shukla, D. (2017). Zinc oxide tetrapods inhibit herpes simplex virus infection of cultured corneas. Mol. Vis. *23*, 26–38.
16. Brovkovych, V., Izhar, Y., Danes, J.M., Dubrovskyi, O., Sakallioglu, I.T., Morrow, L.M., Atilla-Gokcumen, G.E., and Frasor, J. (2018). Fatostatin induces pro- and anti-apoptotic lipid accumulation in breast cancer. Oncogenesis *7*, 66.